Mech. Adv. Technol. Vol. 7, No. 1, 2023, pp. 16–23

DOI: 10.20535/2521-1943.2023.7.1.273332

UDC 629.736.072.8; 681.3

Taking into account a location of aircraft's center of mass during motion cuing

V. V. Kabanyachyi[1] • S. V. Hrytsan[1] • S. S. Yankovskyi[2]

Received: 23 January 2023 / Revised: 20 February 2023 / Accepted: 27 February 2023

Abstract. *Compared to other information sources, motion cues provide a pilot with anticipatory information about spatial position and movement of aircraft. For motion cueing a flight simulator cockpit is installed on a motion system, movement of which motion cueing. Therefore, motion system is one of the most important components of full flight simulators. The problem of effective use of constructive resources of six-degrees of freedom synergistic motion system has been solved. But the problem of improving the motion cueing remained unsolved, due to the fact that location of motion system center of rotation is significantly different from location of aircraf's center of gravity, and motion cues differ from real, flight one. The study subject is motion cueing on flight simulators. The problem was solved on the basis of simplified operator for transformation of motion system movements along individual degrees of freedom into jack movements, cubic spline functions to describe the dependence of the centers of rotation along pitch and yaw, and optimization theory using the deformable polyhedron method. The formulated and solved problem of taking into account of location of aircraft's center of gravity during motion cueing along pitch and yaw increases an efficiency of using of constructive resource of a six-degrees of freedom synergistic motion system, a motion cueing fidelity and training realism on flight simulator.*

Keywords: *flight simulator; six-degrees of freedom synergistic motion system; motion cueing; cubic spline function; constructive resource; aircraft center of mass.*

Introduction

Motion system is a mechanism that creates a feeling of being in a real motion environment and is one of the most important components of a flight simulator (Fig. 1). Among proposed design schemes, the scheme proposed by Stewart [1] (Fig. 2) turned out to be the most effective when using heavy cockpits of modern non-maneuvering aircraft and the need to ensure linear movement ranges of motion system over 1 m and angular – 25 degrees.

The Stewart platform is six degrees of freedom (6-DOF) parallel mechanism. The Stewart platform consists of a fixed base and a triangular rigid body movable platform connected together by six independently actuated extensible jacks, each spherical joints at both ends or with a spherical joint at one end and with universal joint at the other. Although joint positions can be arbitrary, evenly spacing them results in special cases. When a pair of jacks share the same joint spaced 120° on the movement platform, this is called a 6–3 configuration. The motions of the Stewart platform are composed of translation and rotation motions. The translation motions are defined as longitudinal, lateral and vertical. The rotation motions are defined as the rolling, the pitching and the yawing. Position and orient of movable platform are obtained by varying jack lengths.

Since a parallel structure is a closed kinematics chain, all jacks are connected from the origin of the tool point by a parallel connection. This connection allows a higher precision and a higher velocity. Due to the parallel structure, the payload is distributed to the six jacks so that the platform offers high rigidity, high force-to-weight ratio, high positioning accuracy, and low movement inertia.

Parallel kinematic mechanisms have better performance in terms of a high degree of accuracy, high speeds or accelerations and high stiffness. It possess properties like low speed and large payload conditions. The development of products and equipment with high precision, high density, and high reliability is a major trend in the current era. So, due to these advantageous properties, they seem

✉ *V. V. Kabanyachyi*
vkabanyachyi@ukr.net

[1] *Igor Sikorsky Kyiv Polytechnic Institute, Kyiv, Ukraine*

[2] *Antonov State Enterprise, Kyiv, Ukraine*

perfectly suitable for industrial high-speed applications, such as pick-and-place or micro and high-speed machining. They are used in many fields such as flight simulation, motion base of classical automotive, surgical robots, entertainment devices, machine tools, haptic devices, radio telescope, remote surveillance devices, manufacturing, architectural structures, rehabilitation processes, inspection, vibration isolation, driving simulator and stabilizers, high-precision positioning devices, micromanipulator applications, 3D printing, medical applications, and for various applications in the marine oceanic area.

Fig. 1. Modern flight simulator

The Stewart platform was first reported in a paper by V. E. Gough in 1956 [2]. Eric Gough established a closed-loop kinematic mechanism and its principles in 1947 and built a prototype for tire testing in 1955. In the 1960s, the rise of aeronautics created a demand for flight simulators. D. Stewart published "A Platform with Six Degrees of Freedom" in 1965 [1], discussing a triangular parallel mechanism design approach for the simulators.

The purpose of using of flight simulators while training pilots is to minimize training losses and training time. A parallel mechanism placed under the simulator provides the translation and rotation movements that pilot would be exposed to when flying with a real aircraft. It puts a simulator cockpit in motion, which creates a perception of movement along six degrees of freedom for pilots, as in a real flight.

Many techniques [3–23] have been proposed to solve different aspects of motion systems. But only one investigation [3] was aimed on optimal use of structural resources of motion system. The results of this calculations [3] show that structural resources of motion system along the linear degrees of freedom are not fully used. The unused constructive resource is determined by a mismatch between allowable motion system movement (Fig. 3, 4, 5, curves 1) and operating movement range of motion system (Fig. 3, 4, 5, curves 3) for a same degrees of freedom. It is desirable that a constructive resource of motion system is used in full and values of allowable motion system movements are equal to values of corresponding operating movement ranges.

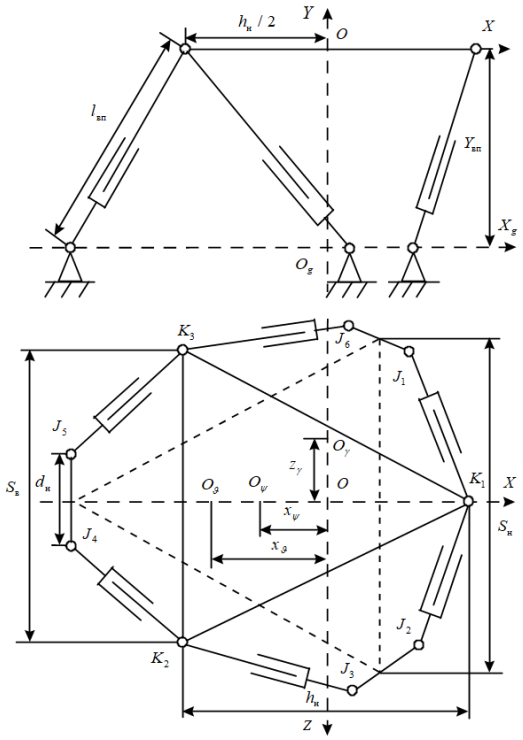

Fig. 2. A schematic diagram of Stewart platform

The purpose and objectives of the study

To motion cueing as close as possible to the real ones, linear and angular accelerations at pilot's seat location should be calculated:

$$\ddot{s}_{ЛАy} = \left(n_y - \cos\vartheta_a \cos\gamma_a\right) g + L_{кр}\dot{\omega}_x$$

$$\ddot{s}_{LAz} = n_z g - L_{кр}\dot{\omega}_y$$

where $\ddot{s}_{LAy}$, $\ddot{s}_{LAz}$ are respectively vertical and lateral aircraft acceleration at pilot's seat location;

n_y, n_z are respectively vertical and lateral overload in aircraft's center of gravity;

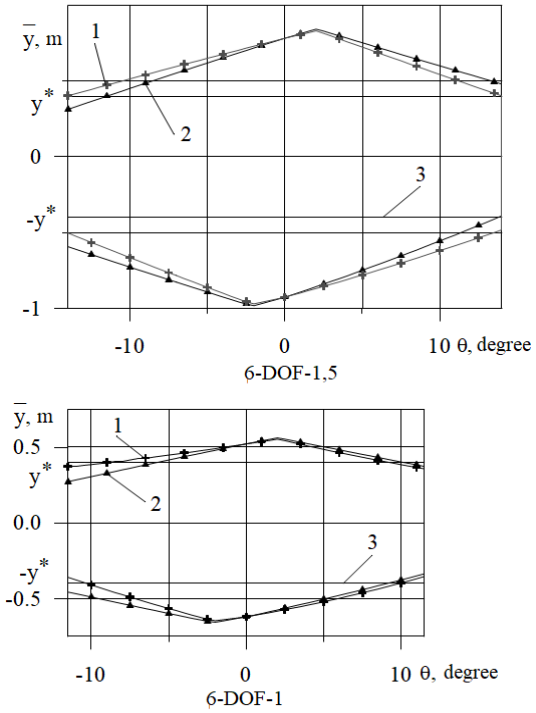

Fig. 3. Allowable motion system movement (1), traditional approach (2), and operating movement range of motion system (3) along vertical degree of freedom

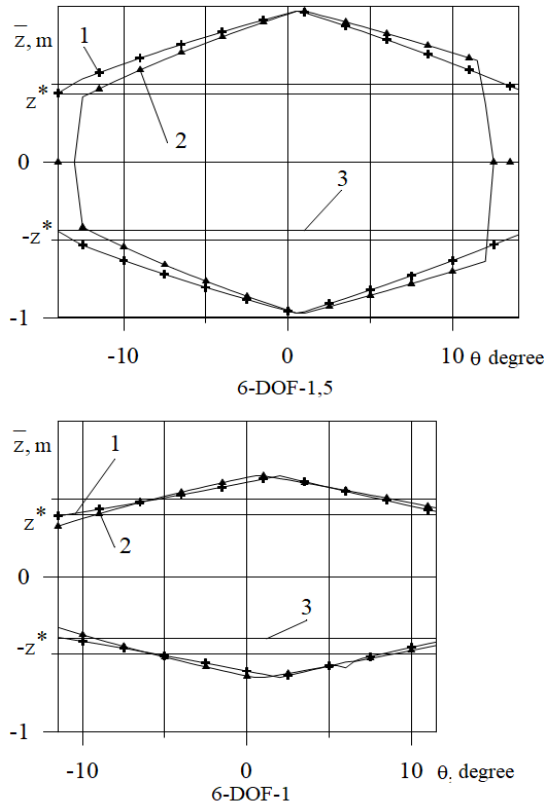

Fig. 4. Allowable motion system movement (1), traditional approach (2), and operating movement range of motion system (3) along lateral degree of freedom

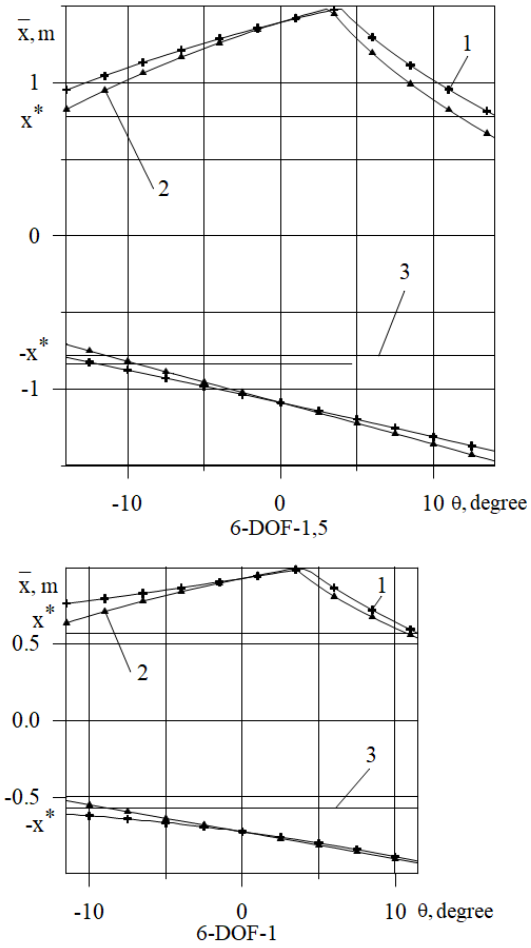

Fig. 5. Allowable motion system movement (1), traditional approach (2), and operating movement range of motion system (3) along vertical degree of freedom

$\dot{\omega}_y, \dot{\omega}_z$ are respectively angular accelerations of yaw and pitch of aircraft; ϑ_a is aircraft pitch angle; γ_a is aircraft roll angle; $L_{кр}$ is distance from aircraft's center of gravity to pilot's seat, measured along the middle fuselage horizontal with aircraft neutral centering.

An aircraft center of gravity is located at a considerable distance from rotation axis of flight simulator cockpit. Flight simulator center rotations are located near pilot's seat location. So motion cues on flight simulators do not reach values of real motion cues. Therefore purpose of the work to take into account a location of aircraft's center of mass in order to increase fidelity of motion cuing.

Methodology of the study

Displacement of flight simulator both pitch and yaw axes in the direction of aircraft's center of gravity provides an increase in linear motion system accelerations due to angular motions. Therefore, if jacks have not reached limits, it is possible to shift axis coordinates of both pitch and yaw

along the longitudinal axis *OX* in such way that they approach coordinates of aircraft center of gravity:

$$x_\vartheta \to x_{ЦМ};$$
$$x_\psi \to x_{ЦМ},$$

where $x_{ЦМ}$ is aircraft center of gravity; x_ϑ, x_ψ is respectively rotation axis of motion system along pitch and yaw.

First of all, introduce (see Fig. 2) the right body system coordinate system *OXYZ* connected to motion system, which beginning *O* is in the plane of upper jacks K_1, K_2, K_3, and the axes *OX*, *OY* and OZ are parallel to the corresponding aircraft axes, and the normal stationary Earth coordinate system $O_gX_gY_gZ_g$, which beginning O_g coincides with the projection of the point *O* on the plane of the lower jacks $J_1, J_2, J_3, J_4, J_5, J_6$ under the condition of equality of jack displacements $l_1 = l_2 = l_3 = l_4 = l_5 = l_6$, and whose axes O_gX_g, O_gY_g and O_gZ_g are parallel to axis *OX, OY* and *OZ* accordingly.

In scalar form, on the basis of the quadratic approximation, which consists in replacing of angle trigonometric functions with angles themselves and preserving only values of the first and second order of smallness, considering angles as small values and taking into account the small range of their changes, the coordinates of the upper rotation center coordinates of jacks in the Earth coordinate system $O_gX_gY_gZ_g$ along the axes O_gX_g, O_gY_g and O_gZ_g $x_в = \{x_{вk}\}$, $y_в = \{y_{вk}\}$, $z_в = \{z_{вk}\}$, $k = \overline{1,6}$, where $x_{вk}$, $y_{вk}$, $z_{вk}$ is respectively the upper rotation center coordinates of *k*-th jacks in the Earth coordinate system $O_gX_gY_gZ_g$ along the axes O_gX_g, O_gY_g and O_gZ_g, are described by the expression:

$$\begin{aligned} x_{вk} &= x + x_{вk}\left[1 - 0,5\left(\psi^2 + \vartheta^2\right)\right] + z_{вk}\left(\vartheta\gamma + \psi\right); \\ y_{вk} &= y + x_{вk}\vartheta - z_{вk}\gamma + \gamma_{вn}; \\ z_{вk} &= z - x_{вok}\psi + z_{вok}\left[1 - 0,5\left(\psi^2 + \gamma^2\right)\right],\ k = \overline{1,6}, \end{aligned} \quad (1)$$

where $x_{вok}$, $z_{вok}$ are respectively the upper rotation center coordinates of *k*-th jacks in the body coordinate system *OXYZ* along the axes *OX*, and *OZ*;

$x, y, z, \gamma, \psi, \vartheta$ are motion system movement along longitudinal, vertical, lateral degrees of freedom, roll, yaw, and pitch;

where $Y_{вn}$ is upper jack coordinate along the vertical axis *OY* in the initial position of the motion systems

$$Y_{вn} = \sqrt{l_{вn}^2 + \left(x_{вk} - x_{нk}\right)^2 + \left(z_{вk} - z_{нk}\right)^2},$$

where $x_{нk}$, $z_{нk}$ are the coordinates of the lower rotation centers of *k*-th jacks in the Earth coordinate system $O_gX_gY_gZ_g$ along the axes O_gX_g and O_gZ_g, $l_{вn}$ is the average jack length, which corresponds to the initial position of motion system and is equal to half of working stroke of jack rods $l_{вn} = (l_{\max} - l_{\min})/2$, where $l_{\max}, l_{\min}$ is respectively, jack length with extremely extended and extremely removed rod, defined as distances between the coordinates of the upper and lower rotation centers of jacks in the direction of jack with fully extended and fully removed rod.

In formula (1) motion system movement along pitch and yaw are linearly related. This allows us to calculate the coordinates of upper rotation centers of jacks with the formulas:

$$\begin{aligned} x_{вk} &= x + x_{вok} - 0,5\left[\left(x_{вok} - x_\psi\right)\psi^2 + \left(x_{вok} - x_\vartheta\right)\vartheta^2\right] + z_{вok}\left(\vartheta\gamma + \psi\right) \\ y_{вk} &= y + \left(x_{вok} - x_\vartheta\right)\vartheta - z_{вok}\gamma + Y_{вn}; \\ z_{вk} &= z - \left(x_{вok} - x_\psi\right)\psi + z_{вok}\left[1 - 0,5\left(\psi^2 + \gamma^2\right)\right], \quad k = \overline{1,6}. \end{aligned}$$

To improve the quality of motion cueing and use efficiency of constructive resources of motion system, working range of motion system movement along pitch $[-\vartheta^*; \vartheta^*]$ is divided into subintervals $[\vartheta_{\vartheta i}; \vartheta_{\vartheta(i+1)}]$, $i = \overline{1, n_\vartheta - 1}$ and $[\vartheta_{\psi i}, \vartheta_{\psi(1+1)}], i = \overline{1, n_\psi - 1,}$ the coordinates of the axes of pitch and yaw are described by cubic spline functions:

$$x_\vartheta = \begin{cases} x_\vartheta^- & \left| \vartheta \le -\vartheta^*; \right. \\ x_\vartheta^- + \dfrac{x_\vartheta^+ - x_\vartheta^-}{2\vartheta^*}\left(\vartheta + \vartheta^*\right) & \left| -\vartheta^* < \vartheta < \vartheta^*; \right. \\ x_\vartheta^+ & \left| \vartheta \ge \vartheta^*, \right. \end{cases}$$

$$x_\psi = \begin{cases} x_\psi^- & \left| \vartheta \le -\vartheta^*; \right. \\ x_\psi^- + \dfrac{x_\psi^+ - x_\psi^-}{2\vartheta^*}\left(\vartheta + \vartheta^*\right) & \left| -\vartheta^* < \vartheta < \vartheta^*; \right. \\ x_\psi^+ & \left| \vartheta \ge \vartheta^*, \right. \end{cases}$$

here $-\vartheta, \vartheta$ is respectively a maximum negative and positive value of working range of motion system movement along pitch;

$x_\vartheta^-, x_\vartheta^+, x_\psi^-, x_\psi^+$ are respectively coordinates of pitch and yaw axes of motion system movement along the longitudinal axis *OX*, which correspond to negative and positive limit values of working range of motion system movement along pitch.

$\vartheta_{\vartheta i}, \vartheta_{\psi i}$ is respectively *i*-th point of division of working range of motion system movement along the pitch $[-\vartheta^*, \vartheta^*]$ into subintervals $[\vartheta_{\vartheta i}; \vartheta_{\vartheta(i+1)}]$, and $[\vartheta_{\psi i}, \vartheta_{\psi(i+1)}]$, $i = \overline{1, n_\psi - 1}$; i is an index of division point of working range of motion system movement along the pitch;

n_ϑ, n_ψ is respectively, a number of division points of working range of motion system movement along the pitch $[-\vartheta^*, \vartheta^*]$ into subintervals $[\vartheta_{\vartheta i}; \vartheta_{\vartheta(i+1)}], i = \overline{1, n_\vartheta - 1}$ and $[\vartheta_{\psi i}, \vartheta_{\psi(i+1)}]$, $i = \overline{1, n_\psi - 1}$;

$x_{\vartheta i}, x_{\psi i}$ are respectively, coordinates of the pitch and yaw axis of motion system along the longitudinal axis *OX* at the

i-th division point of working range of motion system movement along the pitch $[-\vartheta^*,\vartheta^*]$ into subintervals

$[\vartheta_{\vartheta i};\vartheta_{\vartheta(i+1)}]$, $i=\overline{1,n_\vartheta-1}$ and $[\vartheta_{\psi i},\vartheta_{\psi(i+1)}]$, $i=\overline{1,n_\psi-1}$;

$M_{\psi i}=\ddot{x}_\psi\left(\vartheta_{\psi i}\right), M_{\vartheta i}=\ddot{x}_\vartheta\left(\vartheta_{\vartheta i}\right)$ are constant coefficients;

$h_{\vartheta i}=\vartheta_{\vartheta(i+1)}-\vartheta_{\vartheta i}, h_{\psi i}=\vartheta_{\psi(i+1)}-\vartheta_{\psi i}$ are breakdown steps, and are shifted in the direction of aircraft center of gravity and are the coordinate values of the pitch and yaw axes of the motion system movement along the longitudinal axis OX at division points of working range of motion system movement $\{x_\vartheta\}$ and $\{x_\psi\}$ and constant coefficients of cubic spline functions $\{M_\psi\}$ and $\{M_\vartheta\}$.

In order to effectively solve the problem of determining the working ranges of motion system movements, it is necessary to take into account the peculiarities of piloting and perception of motion cueing along degrees of freedom. The set of kinematically possible movements of motion system is given in the form of region of possible positions of motion system in the n-dimensional space of n composite coordinates. The following ranges of motion system movements are minimum required:

– for motion cueing along the longitudinal, vertical and lateral degrees of freedom $x_{\min}=y_{\min}=z_{\min}=0.4m$;

– for motion cueing along the roll $\gamma_{\min}=5$ degrees;

– for motion cueing along the roll and static motion cueing along the lateral degree of freedom $\gamma_{\Sigma\min}=10$ deg;

– for motion cueing along the yaw $\psi_{\min}=4$ degrees;

– to simulate an aircraft pitch and static motion cues along the longitudinal degree of freedom $\vartheta_{\min}=9$ deg.

With the maximum use of structural resources of motion system, when axes coordinates of pitch and yaw are shifted in such a way as to ensure maximum working

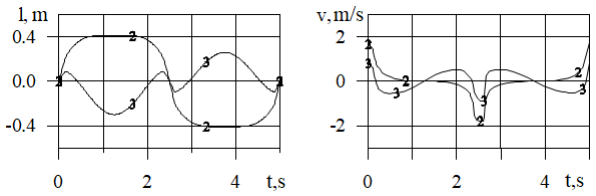

a) traditional approach

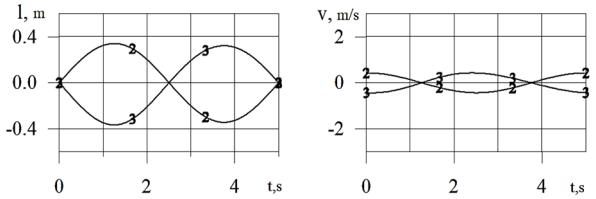

b) developed approach

Fig. 6. Displacement (l) and speed (v) of the 2nd (2) and 3rd (3) jacks

ranges of motion system movements, the task of their determining is reduced to an extreme problem:

$$x^*+y^*+z^*+\vartheta^*\to\max$$
$$\tilde{P}_{s1}\subset\tilde{U}$$
$$\tilde{P}_{s2}\subset\tilde{U}$$
$$\tilde{P}_{s3}\subset\tilde{U}$$
$$x_\vartheta\to x_{LIM}$$
$$x_\psi\to x_{LIM}$$

where $\{s_i^*\}=\{x^*,y^*,z^*,\gamma^*,\gamma_\Sigma^*,\psi^*,\vartheta^*\}$ is respectively working range along longitudinal, vertical, lateral degrees of freedom, and pitch; $\tilde{U}$ is area of possible attitudes of motion system; $\tilde{P}_{s1}$ is parallelepiped which one edge length is equal to a minimum required range of motion system movement along the yaw, and which two other edge lengths are not less than minimum required ranges of motion system movement along the pitch and longitudinal degrees of freedom

$$\tilde{P}_{s1}=\left\{(y,\vartheta,\psi)\middle|x^*\ge x_{\min},\vartheta^*\ge\vartheta_{\min},-\psi_{\min}\le\psi\le\psi_{\min}\right\};$$

is parallelepiped in which one edge length is equal to minimum required range of motion system movement along the roll, and which two other edge lengths are not less than minimum required ranges of motion system movement along the pitch and vertical degrees of freedom

$$\tilde{P}_{s2}=\left\{(y,\vartheta,\gamma)\middle|y^*\ge y_{\min},\vartheta^*\ge\vartheta_{\min},-\gamma_{\min}\le\gamma\le\gamma_{\min}\right\};$$

$\tilde{P}_{s3}$ is hyperparallelepiped which two edge lengths are equal to minimum required ranges of motion system movement along the roll and yaw, and which two other edge lengths are not less than minimum required ranges of motion system movement along the pitch and lateral degrees of freedom

$$\tilde{P}_{s3}=\left\{(y,\vartheta,\gamma_\Sigma,\gamma)\middle|z^*\ge z_{\min},\vartheta^*\ge\vartheta_{\min},\right.$$
$$\left.-\gamma_{\Sigma\min}\le\gamma_\Sigma\le\gamma_{\Sigma\min},-\psi_{\min}\le\psi\le\psi_{\min}\right\}.$$

The geometric meaning of this problem is to fit into the area of possible attitudes of the motion system $\tilde{U}$ alternately three parallelepipeds. The working ranges of motion system movements along the pitch, longitudinal, vertical, and lateral degrees of freedoms, dependence of axes coordinates of the pitch, and yaw on a pitch angle are searched.

Results and their discussion

The results of calculations in Fig. 6, 7 and 8–10 (curves 2), which were carried out by the method of a deformable polyhedron, show:

– along the longitudinal degree of freedom constructive resource of motion system movement is significant and cannot be fully utilized;

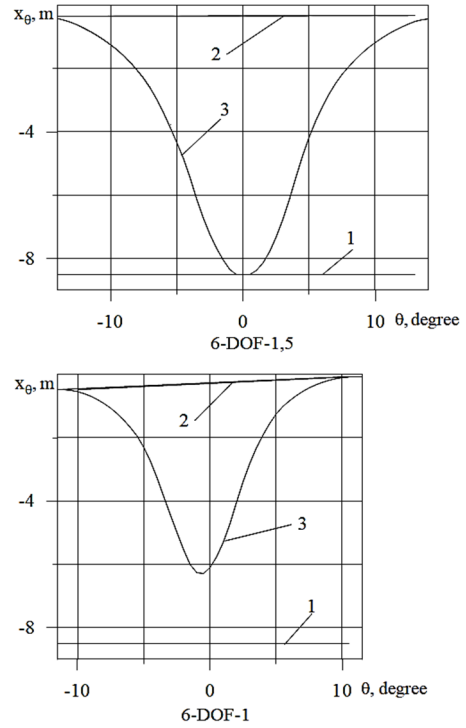

Fig. 7. Coordinates of aircraft center of mass (1), linear dependencies of the coordinates of the pitch axes on the pitch angle (2) and described by cubic spline functions (3)

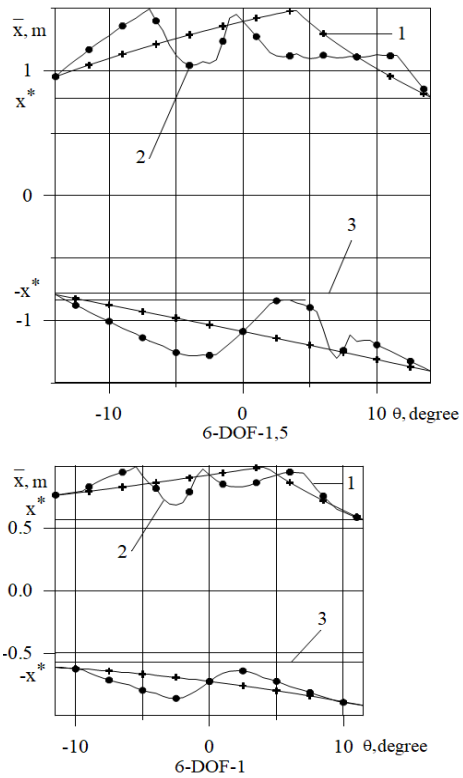

Fig. 8. Acceptable movements with linear (1) and cubic spline functions (2) dependencies of the pitch and yaw axes coordinates and maximum working ranges of motion system movements (3) along longitudinal degree of freedom

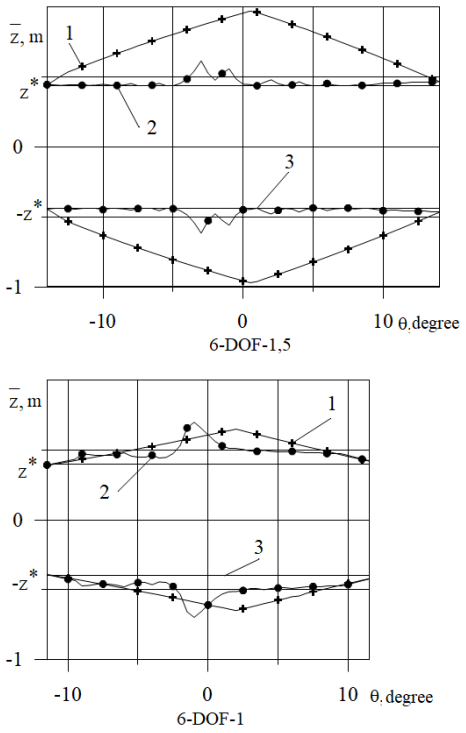

Fig. 9. Acceptable movements with linear (1) and cubic spline functions (2) dependencies of the pitch and yaw axes coordinates and maximum working ranges of motion system movements (3) along vertical degree of freedom

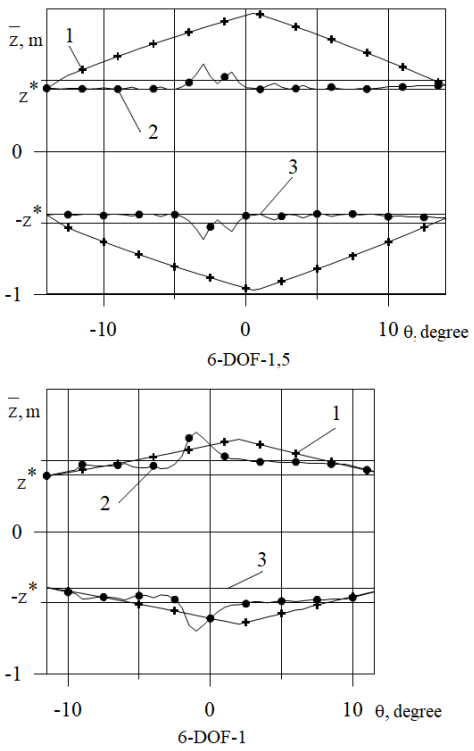

Fig. 10. Acceptable movements with linear (1) and cubic spline functions (2) dependencies of the pitch and yaw axes coordinates and maximum working ranges of motion system movements (3) along lateral degree of freedom

– restrictions along vertical and lateral degree of freedom are active;

– due to significant constructive resource, the pitch axis in motion system with 1.5 m jacks is shifted towards aircraft's center of gravity in the entire range of angles of the motion system movement, and in the range of angles 2 degrees almost coincides with aircraft's center of gravity, which significantly approximates a motion perception on flight simulator and aircraft.

– The movements and velocities of the most charac-teristic 2nd and 3rd of motion system with 1.5 m jacks and sinusoidal program signal with an amplitude of 14 degrees and a frequency of 0.2 Hz, which are shown in Fig. 6, show that compared to the traditional approach (Fig. 6, *a*) with maximum use of structural resources of the motion system (Fig. 9, *b*):

– the maximum movements of jacks have changed little: the maximum movements of the 2nd jack have increased by 18%, and the 3rd - decreased by 19%;

– the nature of jacks movements has essentially changed: there are shelves at movement of the 2nd jack, and there are changes in the direction at movement of the 3rd jack;

– the maximum speeds of jacks have increased almost 5 times.

Conclusions

Developed methodology takes into account a location of aircraft's center of mass, uses simplified operator for transformation of motion system movements along individual degrees of freedom into jack movements, cubic spline functions to describe dependencies of rotation centers of both pitch and yaw and optimization theory using the deformable polyhedron. Due to this it increases an efficiency of using of constructive resource of six degrees of freedom synergistic motion system and training realism on flight simulator as simulated motion cues closer to real one.

References

[1] D. A. Stewart "Platform with Six Degrees of Freedom", in *Proc. of the Institution of mechanical engineers*, Part–I, Vol. 180, No. 15, pp. 371–386, 1965. doi: http://dx.doi.org/10.1243/PIME_PROC_1965_180_029_02

[2] V.E. Gough "Contribution to discussion of papers on research in automobile stability", *Control and tyre performance*, Vol. 171, pp. 392–395, 1956.

[3] V.V. Kabanaychyi, "Permissible and optimal working ranges of displaced of six-degrees-of-freedom motion system", *Cybernetics and computer technology*, Issue 136, p. 61–68, 2002.

[4] S.S. Ahmadi and A. Rahmanii, "Nonlinear model predictive control of a Stewart platform based on improved dynamic model", *Int. J. Theor. Appl. Mech*, No. 5, pp. 18–26, 2020.

[5] Diego Silva, Julio Garrido and Enrique Riveiro, "Stewart Platform Motion Control Automation with Industrial Resources to Perform Cycloidal and Oceanic Wave Trajectories", *Machines*, No. 10, pp. 1–28, 2022, doi: 10.3390/machines10080711

[6] Fengchao Liang, Shuang Tan, Xiaolin Zhao, Jiankai Fan, Zhe Lin, Zhicheng Shi and Xiaojun Kang, "Kinematics and Dynamics Simulation of a Stewart Platform", *Journal of Physics*, pp. 012–026, 2022. doi: 10.1088/1742-6596/2333/1/012026

[7] D.E. Galván-Pozos, F.J. Ocampo-Torres, "Dynamic Analysis of a Six-Degree of Freedom Wave Energy Converter Based on the Concept of the Stewart-Gough Platform", Renew. Energy, No. 146, pp. 1051–1061, 2020. doi: 10.1016/j.renene.2019.06.177

[8] C. Gosselin, J-P. Merlet, "Parallel robots: Architecture, modeling, and design", *Encyclopedia of robotics*, Berlin, Heidelberg: Springer Berlin Heidelberg, 2020, pp. 1–6. https://doi.org/10.1007/978-3-642-41610-1_158-1

[9] Javier Velasco, Isidro Calvo, Oscar Barambones, Pablo Venegas and Cristian Napole, "Experimental Validation of a Sliding Mode Control for a Stewart Platform Used in Aerospace Inspection", *Applications Mathematics*, pp 1–15, 2020. doi: 10.3390/math8112051

[10] J. Jiao, Y. Wu, K. Yu, R. Zhao, "Dynamic modeling and experimental analyses of Stewart platform with flexible hinges", *J. Vib. Control*, No. 25, pp. 151–171, 2019. DOI: 10.1177/1077546318772474

[11] Y.S. Kim, H. Shi, N. Dagalakis, J. Marvel, G. Cheok, "Design of a six–DOF motion tracking system based on a Stewart platform and ball–and–socket joints", *Mech. Mach. Theory*, No. 133, pp. 84–94, 2019. DOI: 10.1016/j.mechmachtheory.2018.10.021

[12] S. Kizir, Z. Bingül, "Design and development of a Stewart platform assisted and navigated transsphenoidal surgery" *Turk. J. Electr. Eng. Comput. Sci*, No. 27, pp. 961–972, 2019. DOI: 10.3906/elk-1608-145

[13] Z.Q. Lu, D. Wu, H. Ding, L.Q. Chen, "Vibration isolation and energy harvesting integrated in a Stewart platform with high static and low dynamic stiffness", *Appl. Math. Model*, No. 89, pp. 249–267, 2021. DOI: 10.1016/j.apm.2020.07.060

[14] S. Pedrammehr, S. Nahavandi, H. Abdi, "Closed–form dynamics of a hexarot parallel manipulator by means of the principle of virtual work", *Acta Mech. Sin*, No. 34, pp. 883–895, 2018.

[15] S. Shastry, R. Avaneesh, K. Desai, S. Shah, "Optimal design of a Stewart–Gough platform for multidirectional 3-D printing", *Precision Product-Process Design and Optimization*, Singapore: Springer Singapore; 2018, pp. 1–29, DOI: 10.1007/978-981-10-8767-7_1

[16] M. Shariatee and A. Akbarzadeh, “Optimum dynamic design of a Stewart platform with symmetric weight compensation system”, *J. Intell. Robot. Syst*., No. 103, pp. 55–66, 2021. DOI: 10.1007/s10846-021-01461-8

[17] T.S. Tamir *et al*., “Design and Optimization of a Control Framework for Robot Assisted Additive Manufacturing Based on the Stewart Platform”, *Int. J. Control Autom. Syst*, No. 20, pp. 968–982, 2022. DOI: 10.1007/s12555-021-0058-4

[18] Trent Peterson, “Design and implementation of stewart platform robot for robotics course laboratory”, Ph.D. dissertation, San Luis Obispo. March 2020

[19] D. Xiaolin *et al*., “Modal space neural network compensation control for Gough-Stewart robot with uncertain load”, *Neurocomputing*, No. 449, pp. 245–257, 2021. DOI: 10.1016/j.neucom.2021.03.119

[20] X. L. Yang *et al*., “Dynamic modeling and decoupled control of a flexible Stewart platform for vibration isolation”, *J. Sound Vib*, 439, pp. 398–412, 2019. DOI: 10.1016/j.jsv.2018.10.007

[21] R.V. Virgil Petrescu *et al*., “Inverse kinematics of a Stewart platform”, *J. Mechatron. Robot*, No. 2, pp. 45–59, 2018. DOI: 10.3844/jmrsp.2018.45.59

[22] Youjian Liang *et al*., “Kinematics of Stewart Platform Explains Three-Dimensional Movement of Honeybee’s Abdominal Structure”, *Journal of Insect Science*, No. 4, pp. 1–6, 2019. DOI: 10.1093/jisesa/iez037

[23] H. Yun *et al*., “Development of an isotropic Stewart platform for telescope secondary mirror”, *Mech. Syst. Signal Process*, No. 127, pp. 328–344, 2019. DOI: 10.1016/j.ymssp.2019.03.001

Врахування розташування центра мас літака при імітації акселераційних впливів

В.В. Кабанячий[1], С.В.Грицан[1], С.С. Янковський[2]

[1] КПІ ім. Ігоря Сікорського, Київ, Україна
[2] Державне підприємство “Антонов”, Київ, Україна

Анотація. *Порівняно з іншими джерелами інформації акселераційні впливи забезпечують пілота випереджальною інформацією про просторове положення і рух літака. Для імітації акселераційних впливів кабіна тренажера встановлюється на динамічному стенді, переміщення якого імітують акселераційні впливи. Тому динамічний стенд є одним з найважливіших складових комплексних тренажерів літаків. Вирішена проблема ефективного використання конструктивних ресурсів шестистепеневих динамічних стендів опорного типу. Але не вирішеною залишалася проблема поліпшення імітації акселераційних впливів, обумовлена тим, що розташування центра обертання динамічного стенда суттєво відрізняється від розташування центра мас літака, а імітовані акселераційні впливи відрізняються від реальних, польотних. Предметом дослідження є імітація акселераційних впливів на авіаційних тренажерах. Проблема розв’язувалась на засадах спрощеного оператора перетворення переміщень динамічного стенду за окремими степенями вільності в переміщення силових гідроприводів, використання кубічних сплайн-функцій для опису залежностей центрів обертання за тангажем і рисканням та теорії оптимізації з використанням методу деформовного багатогранника. Сформульована і розв’язана задача врахування розташування центра мас літака через наближення центрів обертання динамічного стенду до центра мас літака при імітації акселераційних впливів за тангажем і рисканням підвищує ефективність використання конструктивного ресурсу шестистепеневого динамічного стенду опорного типу, якість імітації акселераційних впливів та реалістичність навчання на авіаційному тренажері.*

Ключові слова: *авіаційний тренажер; шестистепеневий динамічний стенд опорного типу; імітація акселераційних впливів; кубічна сплайн-функція; конструктивний ресурс; центр мас літака.*